Multi-Spectral Image Resolution Refinement using Stationary Wavelet Transform

M. Beaulieu, S. Foucher, L. Gagnon
Centre de Recherche Informatique de Montréal
550 Sherbrooke Street West, Suite 100, Montreal (PQ), Canada, H3A 1B9

***Abstract*- This study presents a pixel-level fusion method to refine the resolution of a multi-spectral image using a high-resolution panchromatic image. Our approach is an adaptation of the ARSIS method that takes into account the higher-order statistical moments of the wavelet coefficients and allows processing of non-dyadic images.**

I. Introduction

This paper presents a fusion method to refine the resolution of a multi-spectral (MS) image using a high-resolution panchromatic (PAN) image and the Stationary Wavelet Transform (SWT), also known as the "à trous" algorithm. Our approach is an adaptation of the ARSIS method that takes into account higher-order statistical moments of the wavelet coefficients and allows the processing of non-dyadic images. The objective is to produce an artificial high-resolution MS image that has nearly the same statistical properties than the original multi-spectral image with no blocking image artifacts.

Pixel-level fusion has proven to be a powerful method for the refinement of the spatial resolution of MS images using PAN [1,2]. Some algorithms operate only in the spatial domain as the PCA, IHS, Brovey and multiplicative methods. These conventional approaches produce good looking color composite but distort the spectral characteristics of the original MS image. New algorithms exploiting the multi-resolution analysis (MRA) framework [3] have been proposed that better preserve the spectral information [4,5]. These algorithms are based on the injection of high-frequency components from the PAN image into the MS image. They provide superior performance [6] for the refinement of the spatial resolution of MS image and can simulate real MS images acquired at higher spatial resolution.

The paper is organized as follows. In Section II, we review the ARSIS method and present our adaptation of it. Section III describes the methodology used in this work while Section IV presents fusion results on real multi-spectral images.

II. The ARSIS method and its adaptation

In the ARSIS method the PAN image is first wavelet-transformed (using a DWT) on two levels. The first level of details $W_{PAN}^{1,k}$, where k stands for the three wavelet coefficient blocks (i.e. horizontal, vertical and diagonal), represents the information to inject in the multi-spectral image XS_i in order to refine the resolution. To do so, the XS_i images are wavelet-transformed on one level. Statistical models relating the second level of wavelet coefficients $W_{PAN}^{2,k}$ to the first level wavelet coefficients $W_{XS_i}^{1,k}$ are built for each block. Those models are used to compute the first level of details $W_{XS_i^{HR}}^{1,k}$ of the wavelet-transformed MS image.

A. Adjusting Marginal Statistics

The simplest model used in the ARSIS method is the adjustments of the first ($\mu_1(x)$) and second moments ($\mu_2(x)$) of the wavelet coefficient statistics according to

$$W_{XS_i^{HR}}^{1,k} = \sqrt{\frac{\mu_2\left(W_{XS_i}^{1,k}\right)}{\mu_2\left(W_{PAN}^{2,k}\right)}} \times \left(W_{PAN}^{1,k} - \mu_1\left(W_{PAN}^{2,k}\right)\right) + \mu_1\left(W_{XS_i}^{1,k}\right) . \qquad (1)$$

This model is a projection of one data set to the other. As a generalization, higher-order moments (μ_3 and μ_4) of the histogram of $W_{PAN}^{1,k}$ can be tuned by adjusting the skewness and kurtosis with those of $W_{XS_i}^{1,k}$. The procedure to accomplish this is described in [7] and is based on the gradient projection of one data set histogram one the other one.

B. Adjusting Joint Statistics

In order to take into account the correlation of the wavelet coefficients between different orientations and scales, the cross-correlation of $W_{PAN}^{1,k}$ is adjusted with the cross-correlation of $W_{XS_i}^{1,k}$ at all orientations k and with the cross-correlation between the $W_{XS_i}^{1,k}$ and their coarser scale $W_{XS_i}^{2,k}$ [7].

C. Adjusting Low Frequencies

In addition, we also need to adjust each multi-spectral band XS_i in order to retrieve the first level of approximations $W_{XS_i^{HR}}^{1,l}$ of the wavelet-transformed image XS_i. In order to compute $W_{XS_i^{HR}}^{1,l}$ from XS_i, we compute the gain G of the low-pass block and multiply XS_i by G.

D. Stationary Wavelet Transform

Two drawbacks of the DWT can be pointed out. First, DWT is not translation-invariant. As a result, misalignments between wavelet coefficients of the MS and PAN subbands may lead to block artifacts and aliasing effects during the reconstruction process. Second, DWT can be used only on images of dyadic size. We get rid of those restrictions by using the Stationary Wavelet Transform (SWT) [8].

III. METHODOLOGY

A. Data Set

Some conditions must be satisfied for the low- and high-resolution images before any pixel-level fusion procedures: (1) images must have different spatial and spectral resolutions, (2) they must be accurately co-registered and (3) no major change must be visible if the images are not acquired at the same time.

The data set used to test our fusion procedure consists of a tandem PAN-XS of 10- 20 m/pix acquired at the same moment by SPOT-1 over the Montreal region (PQ, Canada). The images have been co-registered with a *RMS* error less than 1 pixel. The Digital Count (*DC*) of the PAN was adjusted to take into account the relative sensibilities of the green and red bands of the MS image.

B. Fusion Procedure

Our fusion method is implemented in four steps : (1) the images are wavelet-transformed using the SWT scheme with a number of levels *N* proportional to the spatial resolution ratio between the PAN and MS images, (2) the first level of details $W_{XS_i^{HR}}^{1,h}$, $W_{XS_i^{HR}}^{1,v}$ et $W_{XS_i^{HR}}^{1,d}$ of the XR_i^{HR} wavelet-transformed image are computed from the adjustment of the marginal and joint statistics of the first level of details $W_{PAN}^{1,h}$, $W_{PAN}^{1,v}$ and $W_{PAN}^{1,d}$, (3) the low-frequency subband $W_{XS_i^{HR}}^{1,l}$ is computed from the *DC* of the XS_i images by multiplying the *DC* by the gain of the wavelet filters, (note that the XS_i images have been scaled to fit the dimension of the PAN), and (4) the artificial high-resolution MS image is produced by applying the inverse SWT to the artificial MS wavelet-transformed image.

C. Image Quality Evaluation

The criteria described in [5] are used to evaluate the quality of the fusion with respect to the spectral information content: (1) the artificial MS image should be identical to the original MS image, once it is degraded to the resolution of the original MS image, (2) the artificial MS image computed from a data set for which the spatial resolution has been degraded by a factor of two should be identical to the original MS image. A global quality index (*GQ)* is calculated from the results of both tests according to the following. For each bands (index *i*), one computes the Root Mean Square Error (*RMSE*)

$$RMSE_i = \sqrt{\frac{1}{M \times N} \sum_{i=1}^{M} \sum_{j=1}^{N} \left(XS_i(i,j) - XS_i'(i,j) \right)^2} \quad , \quad (2)$$

and the following *GQ* index:

$$GQ = 1.0 - \frac{\sqrt{\sum_{i=1}^{3} \left(RMSE_i^{TEST1} \right)^2 + \sum_{i=1}^{3} \left(RMSE_i^{TEST2} \right)^2}}{255} \quad (3)$$

IV. RESULTS AND DISCUSSION

A. Wavelets Filters

Our method was tested with symmetric biorthogonal spline wavelets (*Bior*) of various orders *Nr* and *Nd* (*r* for reconstruction, *d* for decomposition) [9]. According to the *GQ* index (Table I), the *Bior1.3* filter provides the best fusion, closely followed by *Bior1.1* (Harr) and *Bior1.5*.

TABLE I

GQ INDEX USING DIFFERENT ORDERS OF BIORTHOGONAL FILTERS

BiorNr.Nd	*GQ*	*GQ (XS1)*	*GQ (XS2)*	*GQ (XS3)*
Bior1.1	*0.9777*	*0.9918*	*0.9919*	*0.9810*
Bior1.3	***0.9780***	***0.9917***	***0.9916***	***0.9814***
Bior1.5	*0.9777*	*0.9915*	*0.9913*	*0.9813*
Bior2.8	*0.9697*	*0.9869*	*0.9872*	*0.9759*
Bior3.9	*0.9679*	*0.9867*	*0.9867*	*0.9740*
Bior4.4	*0.9739*	*0.9886*	*0.9890*	*0.9792*
Bior5.5	*0.9736*	*0.9882*	*0.9883*	*0.9795*
Bior6.8	*0.9734*	*0.9884*	*0.9887*	*0.9789*

B. Statistics Adjustment Scheme

Table II gives the *GQ* index for the following wavelet coefficient statistics adjustments: (1) mean and variance, (2) all marginal statistics (mean, variance, skewness and curtosis), 3) joint statistics, and 4) marginal and joint statistics.

TABLE II

GQ INDEX USING DIFFERENT STATISTICS ADJUSTMENT METHODS

Adjustment	*GQ*	*GQ (XS1)*	*GQ (XS2)*	*GQ (XS3)*
1) Mean & variance	*0.9780*	*0.9917*	*0.9916*	*0.9814*
2) Marginal Statistics	*0.9780*	*0.9917*	*0.9916*	*0.9814*
3) Joint Statistics	*0.9635*	*0.9785*	*0.9794*	*0.9790*
4) Both Statistics	***0.9783***	***0.9915***	***0.9915***	***0.9919***

Results from adjustments "1" and "2" show that higher-order moments have no impact on the fusion. Adjustment "1" provides better results than "3" but adjustment "4" gives the best fusion. The results show that for the computation of only one level of artificial subbands, the impacts of inter-levels and inter-subbands correlation is small.

C. Others Fusion Methods

We compared the best *GQ* result of our method with the ARSIS method (using DWT), the IHS method and two others methods from a Matlab fusion toolbox (SIDWT, PCA) [10].

TABLE III

GQ INDEX OF FUSION USING DIFFERENT FUSION METHODS

Method	*GQ*	*GQ (XS1)*	*GQ (XS2)*	*GQ (XS3)*
1) ARSIS using DWT	*0.9762*	*0.9903*	*0.9904*	*0.9805*
2) Our method using SWT	***0.9783***	***0.9915***	***0.9915***	***0.9819***
3) IHS	*0.8380*	*0.9373*	*0.9456*	*0.9188*
4) SIDWT (fusetool)	*0.9730*	*0.9887*	*0.9881*	*0.9786*
5) PCA (fusetool)	*0.9524*	*0.9797*	*0.9841*	*0.9600*

First, Table III shows that methods "1", "2" and "4" which are based on MRA and injection of high-frequency components, are more efficient for the preservation of spectral information and refinement of the resolution. The IHS and

PCA methods provide good composite images but distort the radiometry. For IHS, the distortion is important and affects the mean and standard deviation considerably.

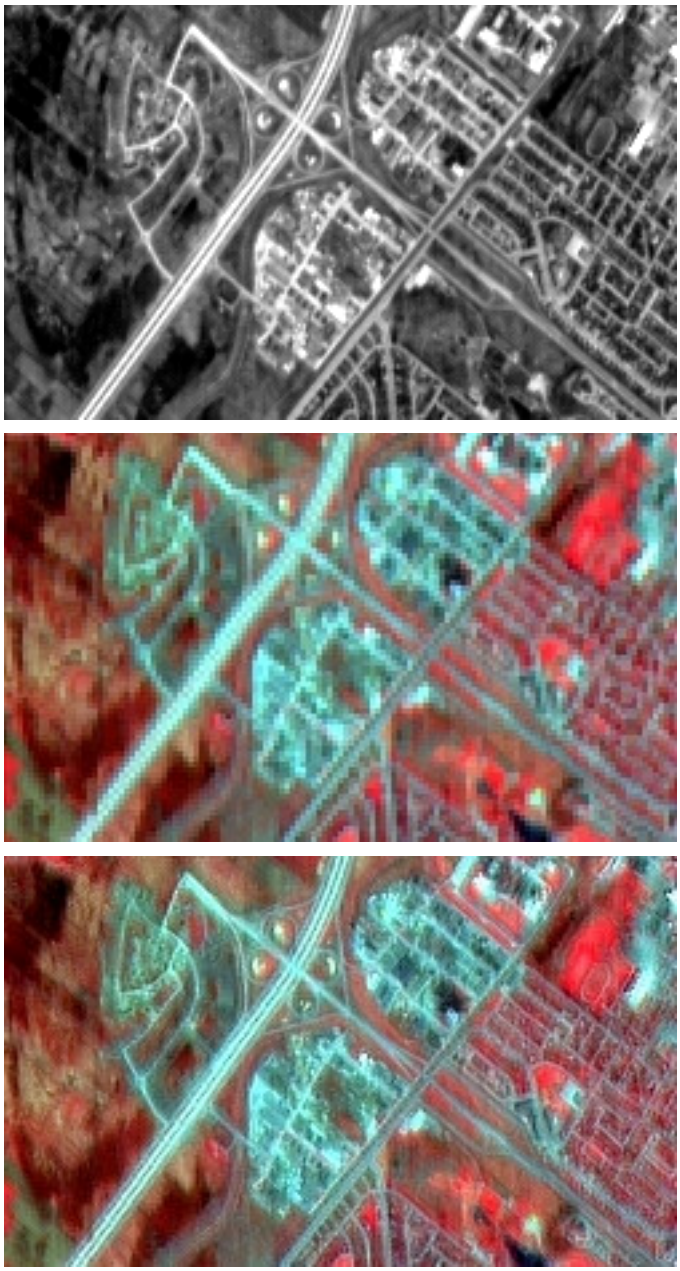

Figure 1. PAN image (up), low-resolution MS image (middle) and artificial high-resolution MS image (bottom)

Second, comparing ARSIS and adjustment "1" in Table II shows the benefit of SWT over the DWT because it is not translation-invariant. Since the SWT is redundant, it averages averaged wavelet coefficients of the MS and PAN subbands leading to a smoother appearance.

Third, column 3, 4 and 5 in Table III show a lower *GQ* index for the fusion of the XS_3 band (infra-red) than for the red and green bands. This is because the spectrum spanned by the PAN sensor (0.51 µm-0.73 µm) does not overlap the IR spectrum (0.79 µm-0.89 µm). It rather overlaps the green (0.50 µm -0.59 µm) and red (0.61 µm-0.68 µm) spectrum. This explain the high correlation between the PAN image and the XS_1 and XS_2 bands. Thus, in the case of SPOT imagery, high-frequencies from the PAN image do not necessary well simulate high-frequencies of a higher-resolution IR sensor. A "good" fusion would rather be achieved when correlation exists between high- and low-resolution images.

Finally, our method using SWT with biorthogonal filters (1,3) and adjustment of the marginal and joint statistics appears to be the best of the four methods tested. Figure 1 shows a visual example of the resolution refinement we obtained with this parameter combination.

V. CONCLUSION

We have presented a fusion method to refine the resolution of a MS image using a high-resolution PAN image and the SWT. The approach is an adaptation of the ARSIS method with the advantage of processing non-dyadic image dimension. It favorably compares to other fusion methods on SPOT imagery, but it can be applied to others combinations of sensors.

ACKNOWLEDGMENTS

This work is supported by the Natural Science and Engineering Research Council (NSERC) of Canada. The authors thank Prof. F. Cavayas, from Université de Montréal, for providing the test images.

REFERENCES

[1] G. Cliche, F. Bonn and P. Teillet, "Integration of SPOT panchromatic channel into its multispectral mode for image sharpness enhancement," Photogr. Eng. and Rem. Sens., vol. 51, no. 3, pp. 311-316, 1985.

[2] P. S. Chavez, S. C. Sides and J. A. Anderson, "Comparison of three different methods to merge multiresolution and multispectral data: Landsat TM and SPOT panchromatic.", Photogr. Eng. and Rem. Sens., vol. 57, no. 3, pp. 295-303, 1991.

[3] S. G. Mallat, "A theory for multiresolution signal decomposition: the wavelet representation", PAMI, vol. 11, pp. 674-693, 1989.

[4] T. Ranchin, "Application de la transformée en ondelette et de l'analyse multirésolution au traitement des images de télédétection.", Thèse de Doctorat, Université de Nice-Sophia Antipolis, France, 146 p., 1993.

[5] Y. Du, P. W. Vachon and J. van der Sanden, "Satellite image fusion with multiscale wavelet analysis for marine applications: preserving spatial information and minimizing artifacts (PSIMA)", Can. J. Remote Sensing, vol. 29, no. 1, pp. 14-23, 2003.

[6] L. Wald, T. Ranchin and M. Mangolini, "Fusion of satellite images of different spatial resolution : Assessing the quality of resulting images", Photogr. Eng. and Rem. Sens., vol. 63, no. 6, pp. 691-699, 1997.

[7] J. Portilla and P. Simoncelli, "A Parametric Texture Model Based on Joint Statistics of Complex Wavelet Coefficients", International Journal of Computer Vision 40(1), pp. 49-71, 2000.

[8] M. Holschneider, R. Kronland-Martinet, J. Morlet and P. Tchamitchian "The "algorithme à trous"" Publication CPT-88/P.2115, Marseille, 1988

[9] I. Daubechies, "Ten Lectures on Wavelet", SIAM, 1992.

[10] O. Rockinger and T. Fechner, "Pixel-level image fusion: the case of image sequences", Proc. SPIE, vol. 3374, pp. 378-388, 1998.